The Impact of Na—H+ Exchange on Long-Term Borosilicate Glass Corrosion: Experiments and Field Observations—9404

J.P. Icenhower, E.M. Pierce, B.P. McGrail
Pacific Northwest National Laboratory
902 Battelle Blvd., MSIN: K6-81
Richland, WA 99352

ABSTRACT

New insights from laboratory experiments coupled with field observations indicate that pore water solutions that eventually breach containment materials in disposal systems will interact with sodium-excess borosilicate waste glass in an unexpected way. Because many glass waste forms are relatively sodium-rich, they are especially vulnerable to Na^+—H^+ exchange (ion exchange or simply, IEX). Although the kinetics of this process has been previously investigated for early-stage glass reactions, the implications of IEX for long-term dissolution resistance have not yet been realized. Non-radioactive glass with major- and minor-element chemical compositions similar to Hanford high-Na waste glass were subjected to dissolution experiments to quantify the rates of matrix dissolution and IEX rates. Single-Pass Flow-Through (SPFT) tests quantified the IEX rate at 40°C pH = 8 and silica saturation and showed a dependence upon the fraction of excess sodium in the glass. The equation for the flux of sodium (in moles released per meter squared per second) dependence on excess sodium is:

$$\log_{10}\text{rate}[\text{mol}/(\text{m}^2\cdot\text{s})] = 0.63R + (-11.0);\ \ r^2 = 0.86$$

where R = molar $Na^+/\Sigma(M^{3+})$. Further, rates of Na release are slower by ≥30% in D_2O-based solutions compared to those in H_2O. These results are the hallmark of IEX reactions. Our results are compared against those from a lysimeter field experiment consisting of glasses buried in Hanford sand and to dissolution experiments conducted with a Pressurized Unsaturated Flow (PUF) apparatus. These longer-term tests indicate an initial decrease in dissolution rate by a factor of 10×, and then a constant steady-state rate thereafter. Thus, these data show that IEX reactions are important at near-saturation conditions and effectively prevent dissolution rates from falling below a minimum value. In sum, IEX modifies the long-term behavior of glass dissolution and models cannot assume that dissolution of Na-rich borosilicate glass will decrease by a factor of 100× to 1000×, as argued for minerals and less sodic glasses.

INTRODUCTION

Integral to the safe storage of nuclear waste is the design of materials that will withstand alteration and release of radionuclide elements when exposed to the geologic environment. If disposal systems can be developed such that radionuclide elements will be immobilized for ten's to hundred's of thousands of years, then a major obstacle for the expanded role of nuclear energy can be overcome. Because of the chemically complex nature of nuclear waste, a fitting design solution is to convert the waste, along with strategically chosen non-radioactive additives, into glass.

Although borosilicate glass has been shown to be a relatively corrosion-resistant waste form for retaining radionuclide elements in short-term laboratory experiments [1-5], concerns persist about the long-term performance of glass. Because weathering of rock forming minerals and natural glasses is slow, it isn't yet clear if laboratory dissolution rates, determined on short duration tests, can be extrapolated to more appropriate geologic time scales. In either case, it is critical to understand the mechanisms by which dissolution occurs so that defensible predictions of rates in

the long term can be established. Laboratory controlled dissolution of silicate minerals has yielded important insights into the reactivity of all silica-based materials, including glass, but as we demonstrate below some of these observations may not fit certain types of glass, especially those that are relatively alkali-rich.

Silicate mineral corrosion reactions have been traditionally described as a series of steps in which each mechanism in the series is dominant over a reaction progress interval [6]. Each step abruptly transitions to the next and the former step is considered to be irrelevant mechanistically during progressive corrosion and reaction. This style of reasoning has also been applied to glass corrosion kinetics, in which the initial step is the reaction alkali ion—hydrogen species exchange (or "IEX"):

$$\text{Si—O—Na} + \text{H}^+ \Leftrightarrow \text{Si—O—H} + \text{Na}^+ \qquad \text{(Eq. 1)}$$

These studies indicate that the exchange reaction is dominant at short reaction times as sodium atoms on the glass surface are selectively removed, but then ceases to be significant as hydrolysis and dissolution reactions become ascendant [7]. More current papers have emphasized that over time, the hydrolysis and dissolution reactions become very slow such that the "long-term" rates decrease from 3 to 4 orders-of-magnitude less than those measured in relatively short-term laboratory experiments. The difference in laboratory and field-derived rates has been highlighted in several papers for both silicate minerals and natural volcanic glasses [8, 9]. These studies conclude that alkali ion—hydrogen species exchange reaction has little impact on the long-term rates that are the principal corrosion processes.

In many glass dissolution studies, the quantity of sodium in glass was balanced by the sum of Al^{3+} or B^{3+}, so that the coupled reaction:

$$^{iv}\text{Si}^{4+} + \square \Leftrightarrow {}^{iv}(\text{Al, B})^{3+} + \text{Na}^+ \qquad \text{(Eq. 2)}$$

(where □ is a "site" vacancy and the superscript "iv" refers to the number of oxygen atoms coordinated to the metal) remains balanced. However, in some glasses, such as those planned to immobilize radioactive elements at Hanford, Washington [10], or Russia [11], the amount of sodium exceeds the sum of aluminum and boron [i.e., molar $Na^+ > \Sigma(Al,B)^{3+}$]. In borosilicate glass, four-fold coordinated boron ($^{iv}B^{3+}$) becomes three-fold coordinated ($^{iii}B^{3+}$), the Si—O—Si network is disrupted, and the sodium atom bonds to a terminal oxygen atom. Sodium atoms attached to these non-bridging oxygen (NBO) atoms are more vulnerable to IEX reactions than those associated with bridging oxygen (BO) atoms. From these observations, we predict that glass compositions with "excess" sodium will be more vulnerable to IEX reactions than those with "balanced" concentrations of sodium [i.e., $Na^+ = \Sigma(Al,B)^{3+}$]. Further, the extent of IEX reaction should be proportional to the relative amounts of BO to NBO or, more simply, the extent to which molar Na^+ exceeds that of $(Al, B)^{3+}$.

This paper describes data acquired from a series of Single-Pass Flow-Through (SPFT) experiments in which a variety of glass compositions, whose chemistries reflect prospective waste glasses for Hanford, Washington, were subjected to dissolution. The input solutions for a set of experiments contained progressively more dissolved silica, and the matrix dissolution rate decreased with increasing dissolved silica. The matrix dissolution rates slow in response to an increase in the silica activity, which diminishes the rate of rupture of the Si—O bond caused by hydrolysis. As the solution approaches saturation with respect to amorphous silica, IEX reactions become important once again. This surprising finding indicates that some glass reaction mechanisms occur in parallel, and are not sequential. For parallel reactions, the fastest

mechanism is the dominant one, so that in this case, when the dominant matrix dissolution rate decreases in response to solution saturation state, the IEX mechanism, which is not governed by solution saturation state, becomes the faster rate. We show that in near silica-saturated solutions the IEX reaction is the mechanism that controls release of elements from glass to solution. The implications are that in near-saturated conditions the solution in contact with alkali-rich glass will increase in pH, causing further increase in dissolution. Under these conditions, we expect that the long-term rates for alkali-rich glass will not decrease drastically (up to four orders-of-magnitude), because of the feedback between IEX and higher pH conditions. Preliminary results from lysimeter field tests on alkali-rich glass compositions and long-term Pressurized Unsaturated Flow (PUF) tests indicate only a small decrease (~10×) in the dissolution rate. Accordingly, assessments of repositories containing alkali-rich glass cannot be assured that very low dissolution rate values, such as those measured in the field on glasses not enriched in Na, will occur.

PREVIOUS WORK AND RATIONALE FOR THIS STUDY

Significant laboratory work has established the importance of IEX reactions in glass. Notable studies include the work of Doremus [7], who was one of the first to note that IEX reactions are a general phenomenon in all glasses at the start of progressive alteration and dissolution. Release of Na^+ to solution was well-described by "parabolic" kinetics, in which release was proportional to the inverse of square root of time. Experiments that utilized pH-stat devices demonstrated that measurable concentrations of hydronium (H_3O^+) were consumed in the reaction [12]. Analysis of the glass near the surface indicated that sodium is depleted, and Nuclear Reaction Analysis (NRA) indicated that H_2O and H^+ were the principal species involved in IEX reactions [13]. Experiments labeled with $D_2{}^{18}O$ and $D_2{}^{17}O$ provided further evidence for IEX and the involvement of H^+ [14]. Pederson [15] noted that the half-life of H^+ is very short, due to its reactivity, and suggested that hydrogen participated with IEX through the infiltration of H_2O into glass. The rate-limiting step appears to be the rupture of the O—H bond to produce a proton (H^+), which exchanges with Na^+ to maintain electrical neutrality. The sodium ion is then free to diffuse through the reaction layer to the aqueous solution.

More recently, McGrail et al. [16] measured the IEX rate in a series of experiments with sodium aluminosilicate glasses in which the Na/Al ratio was designed to vary from unity to values > 1. The glasses were reacted in silica-saturated solutions at ambient temperature and, because matrix dissolution and IEX occurred simultaneously, the matrix dissolution rate was monitored by the release of trace amounts of Mo doped in the glasses. The results showed conclusively that the release of Na^+ to solution could not be accounted for solely by matrix dissolutions. Further experiments in D_2O-labelled solutions indicated an isotopic effect for sodium occurred, but no such effect was noted for Mo release. These data are consistent with the hypothesis that relatively Na-rich glasses are subject to IEX reactions, even when the solution is saturated in silica.

Based on the available experimental data, Ojovan and co-workers calculated the time-scales upon which IEX reactions were likely to dominate [17]. They showed that at the initial stage of reaction, glass released sodium via IEX for tens to hundreds of years at pH and temperature values anticipated for the repository. Further, they reported that IEX processes can be significant when the matrix hydrolysis reaction is suppressed, as in the case of the system approaching silica saturation.

These calculations show the potential importance of IEX reactions on performance assessments analyses for vitreous waste forms, but relatively few studies have been conducted using

borosilicate and boroaluminosilicate glasses. In order to more fully develop models of glass corrosion, we report the experimental findings from nine (9) boro- or boroaluminosilicte glasses in buffered pH solutions at 22°C (room temperature) and silica concentrations from dilute to near-saturated. Experiments in D_2O-bearing silica-saturated solutions indicate an isotopic effect for Na release, without a similar effect for tracers of network dissolution, such as Al and B. The experiments show that the magnitude of IEX depends on the glass composition; namely, the Na:Al,B ratio.

METHODS AND MATERIALS

1. Glass. A total of nine (9) boro- and boroaluminosilicate glass compositions were made by blending reagent grade oxides, carbonates, or hydroxides and melted at 1,500°C for 1 hour in air, then quenched on a stainless steel plate. The chemical compositions of the glasses are listed in Table I. All melts were visually homogeneous and possessed low viscosity when molten, and yielded clear, visibly uniform glass. Glass produced in this way was crushed in a ceramic ball mill to produce the samples of powdered glass used in this study. The crushed glass was then sieved to separate the powders into a variety of size fractions; in this study, the -100, +200 mesh (149 to 75 μm diameter) size fractions were used. The powdered specimens were then sonicated in deionized water (DIW) and rinsed in ethanol to remove any adhering particles outside the desired size fraction. After drying in a 90°C oven for several hours the powders were kept in desiccators until used in an experiment.

Table I. Chemical Compositions of Borosilicate Glasses Used in Experiments

wt%	LAWA33	LAWABP1	LAWA44	LD6-5412	HLP-9	HLP-12	HLP-33	HAN28F	BAS-1
Al_2O_3	11.97	10.00	6.20	12.00	6.84	6.74	4.00	10.15	--
B_2O_3	8.85	9.25	8.90	5.00	12.00	9.63	6.00	2.00	5.71
CaO	--	--	1.99	4.00	0.01	0.01	0.01	2.59	--
Cl	0.58	0.58	0.65	--	0.27	0.27	0.32	0.13	--
Cr_2O_3	0.02	0.02	0.02	--	0.07	0.070	0.09	0.08	--
F	0.04	0.04	0.01	--	0.01	0.010	0.01	0.31	--
Fe_2O_3	5.77	2.50	6.98	--	5.38	9.000	5.90	2.53	--
K_2O	3.10	2.20	0.50	1.46	0.40	0.400	0.47	1.96	--
La_2O_3	--	2.00	--	--	0.00	0.000	0.00	0.00	--
MgO	1.99	1.00	1.99	--	1.47	1.440	1.61	1.18	--
Na_2O	20.00	20.00	20.00	20.00	19.56	19.260	23.00	28.62	22.36
P_2O_5	0.08	0.08	0.03	0.19	0.05	0.050	0.06	1.90	--
SO_3	0.10	0.10	0.10	--	0.07	0.070	0.08	0.30	--
SiO_2	38.25	41.89	44.55	55.91	47.98	47.250	52.00	42.56	71.93
TiO_2	2.49	2.49	1.99	--	2.93	2.890	3.21	3.80	--
ZnO	4.27	2.60	2.96	--	1.47	1.440	1.61		--
ZrO_2	2.49	5.25	2.99	--	1.47	1.440	1.61	0.06	--
Total	100.00	100.00	99.86	98.56	99.98	99.97	99.98	98.17	100.00
Alk/(Al+B+Fe)									
	1.27	1.40	1.41	1.78	1.17	1.21	2.32	3.51	4.40

In general, both chemically-simple (B_2O_3+Na_2O+SiO_2±Al_2O_3) and –complex glasses (up to sixteen components) were synthesized and displayed variations in Na:Al,B ratio (Table I). Chemically simple glasses could be compared against glasses containing more components to ascertain the dependence of IEX, if any, on components other than Al_2O_3, B_2O_3, or SiO_2. The

chemically complex glass compositions are non-radioactive surrogates of likely candidates for radioactive waste disposal at Hanford and are, therefore, highly relevant to this discussion.

2. Single-Pass Flow-Through (SPFT) apparatus. The salient features of the SPFT apparatus used in this study are illustrated in Figure 1. Automated and programmable syringe pumps (Kloehn; model 50300) were used to transfer solution from the input reservoir to the Teflon® Savillex *polytetrafluoroethane* (PTFE) reactors. The syringe pumps could be used to run up to four experiments per pump. This configuration was especially useful when experiments with different flow-through rates were required. Transport of solution from the pumps was accommodated by 1/16th inch (O.D.) Teflon tubing that led to a reactor, which consists of an upper and lower half that screw together to form a 40 mL container. The top half of the reactor contains ports for ingress of input and egress of effluent solution. The powdered glass sample lies at the bottom of the reactor in a thin layer. Therefore, the fluid is not pumped directly through the sample, as in other reactor designs. Effluent was accumulated continuously in collection bottles situated outside the oven. A nitrogen generator continuously supplied N_2 to the reservoir, which prevented dissolution of atmospheric CO_2 that may cause deviations in solution *p*H.

Aliquots of effluent solution were routinely checked to ensure that pH control was maintained during the experiment. A second aliquot of the effluent solution was acidified (*p*H < 2) by spectroscopic grade nitric acid and the chemical composition was analyzed by inductively coupled plasma optical emission spectroscopy (ICP-OES) methods. Typically, three blank solutions were drawn before glass was added to the reactor. The blank solutions were analyzed for background concentrations of elements of interest and, together with analyses of starting solution aliquots, assured us that contamination was not a factor.

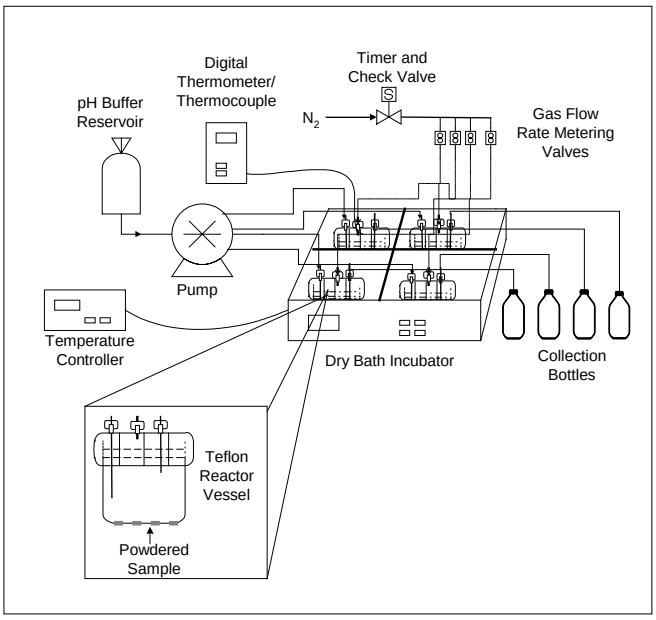

Figure 1. Schematic of Single-Pass Flow –Through (SPFT) Apparatus

Experiments were terminated when the concentrations of elements in the effluent solution became invariant with respect to time (steady-state conditions). Typically, this would take from one to three weeks, depending upon the flow-through rate of the experiments.

3. Solution compositions. Solutions used in these experiments were made by mixing small amounts of the organic THAM (*tris hydroxymethyl aminomethane*) buffer (0.05 M) to deionized water (DIW) and then adding minor concentrations of reagent grade HNO_3 to bring the solution to the *p*H value of 8. Quantities of solid H_4SiO_4 were added to solutions from approximately 0, 20, 40, 60, 80 and 100% saturation with respect to amorphous silica [SiO_2(am)]. The powdered silicic acid was added to the solutions which were kept in an oven at 90°C for one week to ensure that the silica was completely dissolved. The solution *p*H was measured and adjustments were made accordingly.

Deuterium-based solutions were made using commercially-available D_2O. The *p*D (rather than *p*H) of the solution was controlled by mixing small amounts of DCl. Silica-bearing solutions were manufactured by dissolving silicic acid into the D_2O at temperature. Although this resulted in contamination by H, the extent of contamination was small. The relationship between *p*H and *p*D is [12]:

$$p\mathrm{D} = p\mathrm{H} + 0.40 \qquad \text{(Eq. 3)}$$

Solution *p*D values were set to 8. Silica was also added in the manner described above, but only at saturation with respect to SiO_2(am).

4. Rate calculations. Dissolution rates measured using the SPFT apparatus are based on steady-state concentrations of elements in the effluent. Matrix dissolution rates reported herein are normalized to the amount of the element present in the glass by the following formula:

$$r_{i,j} = \frac{(C_{i,j} - \overline{C}_{i,b})q_j}{f_i S_j} \qquad \text{(Eq. 4)}$$

where $r_{i,j}$ is the normalized release rate [g/(m^2·d)] based on element *i* at the j^{th} sampling, $C_{i,j}$ is the concentration (g/L) of the element, *i*, in the effluent at the j^{th} sampling, $\overline{C}_{i,b}$ is the average background concentration (g/L) of the element of interest, q_j is the flow-through rate (L/d) at the j^{th} sampling, f_i is the mass fraction of the element in glass (dimensionless), and S_j is the average surface area (m^2) of the sample over the time period *j-1* to *j*. The detection threshold of any element is defined here as the lowest concentration calibration standard that can be determined reproducibly during an analytical run within 10%. In cases where the analyte is at the detection threshold, the concentration of the element is set at the value of the detection threshold, even though it is likely that the concentration of the element is at a lower value. Flow-through rates were determined by gravimetric analysis of the fluid collected in each effluent collection vessel upon sampling. The value of f_i can be calculated from the chemical composition of the glass.

Quantification of the IEX rate was performed with the recognition that sodium release occurred by two principal mechanisms: a) matrix hydrolysis, and b) IEX. Therefore, in order to distinguish the amount of Na^+ released by matrix dissolution from that of IEX, the matrix dissolution rate, based on release of B, was subtracted from the apparent sodium release rate:

$$\mathrm{IEX} = [\mathrm{rate}_{Na} - \mathrm{rate}_B] \times f_{\mathrm{Na}} / \mathrm{MW}_{\mathrm{glass}} / 86\,400\ [\mathrm{mol}/(\mathrm{m}^2\cdot\mathrm{s})] \qquad \text{(Eq. 5)}$$

where rate_{Na} and rate_B are, respectively, the rate of release of boron and sodium [g/(m^2·d)], f_{Na} (dimensionless) is the mole fraction of Na in glass, $\mathrm{MW}_{\mathrm{glass}}$ is the molecular weight of glass (g/mol), and 86 400 (sec/day) converts units of time from days to seconds.

Dissolution and IEX rate errors were calculated using previously described methods [16].

RESULTS

1. Dissolution in Silica-Amended H_2O Solutions. Concentrations of elements in the effluent (leachate) are listed in Table II. Mass fraction-normalized dissolution rates, based on elemental release, are listed on the right-hand side of Table II.

In nearly every case, the concentrations of Al, B, and Na released from glass decreased as the concentration of dissolved Si increased. The exceptions to this general trend are seen for the results for HAN-28F and BAS-1, in which the concentrations of Na remain the same over the silica concentration interval. Therefore, in general, the dissolution rates of the glasses decreases with increasing silica concentration, as expected from solution saturation arguments.

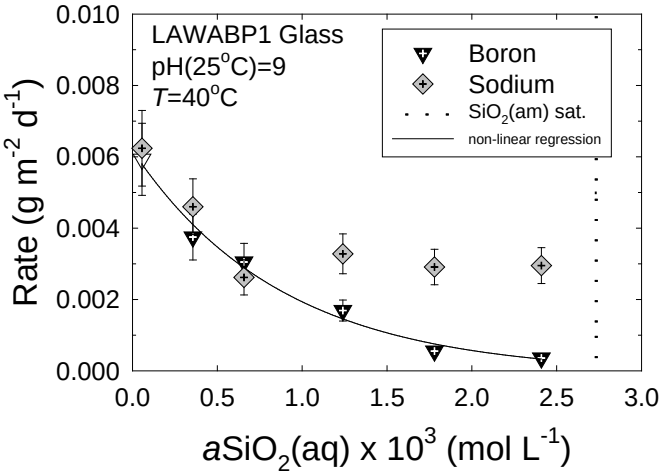

Figure 2. A typical plot of the rate of release of boron and sodium over a silica activity interval. Both Na and B release rates respond to higher activities of silica by decreasing non-linearly. As saturation with respect to SiO_2(am) is approached, Na release rates are faster than those of B, indicating that a second mechanism, apart from hydrolysis and dissolution, is contributing Na to solution. Experiments conducted at *p*H = 8, 40°C.

A typical pattern of boron and sodium release rates as the activity of dissolved silica increases are shown in Figure 2. Both the boron and sodium rates show a similar pattern. In both cases, the rates decrease at low activities of silica, become non-linear, and then approach constant values as the solution saturation state increases. Although B and Na rates overlap at low activities of silica, the two sets of data begin to diverge as silica activity increase. Thus, this figure, along with the data in Table II, illustrates that the network-forming metals, Al and B, decrease rapidly with the input of silica to solution, and then the rates become independent of silica activity.

These data are inconsistent with expectations that glass dissolution rates will decrease linearly in response to increases in silica activity [18]. Further, the relatively rapid release of Na with respect to B is inconsistent with the idea that only matrix dissolution is the mechanism releasing elements into solution at moderate stages of glass corrosion.

Table II. Background-subtracted concentration of Al, B, Na, and Si Released from Glass to Solution at 40°C and *p*H (25°C) = 8 and Normalized Dissolution Rates (2σ error)

Glass I.D.	Conc. Al (μg/L)	Conc. B (μg/L)	Conc. Na (μg/L)	Conc. Si (mg/L)	Normalized rate Al [g/(m^2·d)]	Normalized rate B [g/(m^2·d)]	Normalized rate Na [g/(m^2·d)]
HAN-28F	1,120	125	13,100	3.9	9.73e-3 (2.07e-3)	7.68e-3 (1.74e-3)	2.94e-2 (6.26e-3)
HAN-28F	670	70	10,000	22.6	5.74e-3 (1.23e-3)	3.49e-3 (8.70e-4)	2.23e-2 (4.74e-3)
HAN-28F	393	59	16,000	40.5	1.64e-3 (3.54e-4)	1.33e-3 (3.51e-4)	1.82e-2 (7.74e-3)
HAN-28F	222	47	15,800	54.4	8.88e-4 (1.94e-4)	8.46e-4 (2.60e-4)	1.80e-2 (3.82e-3)
HAN-28F	76	47	16,700	73.0	2.28e-4 (5.56e-5)	8.34e-4 (2.57e-4)	1.88e-2 (4.00e-3)
HAN-28F	--	44	17,200	89.2	--	7.53e-4 (2.43e-4)	1.95e-2 (4.15e-3)
HLP-9	485	479	1,900	3.1	6.08e-3 (2.32e-3)	5.64e-3 (2.17e-3)	5.89e-3 (2.25e-3)
HLP-9	388	376	1,500	11.5	5.03e-3 (1.92e-3)	4.54e-3 (1.76e-3)	4.95e-3 (1.89e-3)
HLP-9	267	278	1,180	21.1	3.44e-3 (1.32e-3)	3.29e-3 (1.20e-3)	3.76e-3 (1.44e-3)
HLP-9	172	223	1,020	40.1	2.13e-3 (8.20e-4)	2.52e-3 (9.95e-4)	3.18e-3 (1.22e-3)
HLP-9	96	148	732	57.5	1.15e-3 (4.49e-4)	1.58e-3 (6.39e-4)	2.25e-3 (8.72e-4)
HLP-9	38	58	496	76.6	3.70e-4 (1.58e-4)	4.25e-4 (2.13e-4)	1.48e-3 (5.80e-4)
HLP-12	578	460	2,190	4.7	7.10e-3 (2.72e-3)	6.65e-3 (2.56e-3)	5.42e-3 (2.26e-3)
HLP-12	418	346	1,700	12.3	5.13e-3 (1.98e-3)	4.99e-3 (1.94e-3)	3.91e-3 (1.71e-3)
HLP-12	353	309	1,550	21.3	4.32e-3 (1.67e-3)	4.46e-3 (1.74e-3)	3.46e-3 (1.54e-3)
HLP-12	203	238	1,200	39.4	2.30e-3 (9.10e-4)	3.28e-3 (1.29e-3)	2.27e-3 (1.11e-3)
HLP-12	199	235	1,430	55.5	2.23e-3 (8.82e-4)	3.22e-3 (1.26e-3)	2.96e-3 (1.36e-3)
HLP-12	116	157	1,300	76.4	1.18e-3 (4.87e-4)	2.03e-3 (8.16e-4)	2.54e-3 (1.21e-3)
LAWA44	396	282	1,640	2.0	6.80e-3 (2.93e-3)	5.37e-3 (2.33e-3)	4.45e-3 (2.14e-3)
LAWA44	400	327	1,880	11.8	6.64e-3 (2.83e-3)	6.10e-3 (2.64e-3)	5.18e-3 (2.43e-3)
LAWA44	292	292	1,570	19.1	5.05e-3 (2.16e-3)	5.68e-3 (2.46e-3)	4.24e-3 (2.05e-3)
LAWA44	162	162	1,130	40.0	2.70e-3 (1.17e-3)	2.89e-3 (1.29e-3)	2.49e-3 (1.35e-3)
LAWA44	100	80	754	57.6	1.63e-3 (7.10e-4)	1.19e-3 (5.72e-4)	1.02e-3 (8.19e-4)
LAWA44	75	47	673	76.5	1.17e-3 (5.16e-4)	4.60e-4 (2.84e-4)	6.87e-4 (7.15e-4)
LAWABP-1	400	171	1,060	1.2	4.14e-3 (7.97e-4)	3.17e-3 (6.17e-4)	3.78e-3 (7.36e-4)
LAWABP-1	192	69	840	10.1	1.83e-3 (3.63e-4)	1.08e-3 (2.24e-4)	2.89e-3 (5.70e-4)
LAWABP-1	133	44	783	22.4	1.22e-3 (2.49e-4)	5.98e-4 (1.36e-4)	2.76e-3 (5.46e-4)

Glass I.D.	Conc. Al	Conc. B	Conc. Na	Conc. Si	Normalized rate Al	Normalized rate B	Normalized rate Na
	(μg/L)	(μg/L)	(μg/L)	(mg/L)	[g/(m^2·d)]	[g/(m^2·d)]	[g/(m^2·d)]
LAWABP-1	103	31	739	39.5	8.83e-4 (1.86e-4)	3.25e-4 (8.81e-5)	2.57e-3 (5.11e-4)
LAWABP-1	83	29	750	57.0	6.60e-4 (1.44e-4)	2.86e-4 (8.16e-5)	2.62e-3 (5.19e-4)
LAWABP-1	74	27	743	79.0	5.28e-4 (1.19e-4)	2.39e-4 (7.22e-5)	2.46e-3 (4.88e-4)
LD6-5412	838	195	2,470	3.3	5.90e-3 (1.13e-3)	5.05e-3 (1.00e-3)	6.87e-3 (1.36e-3)
LD6-5412	523	127	1,620	12.4	3.70e-3 (7.11e-4)	3.10e-3 (6.36e-4)	4.36e-3 (8.90e-4)
LD6-5412	302	77	1,240	23.3	2.03e-3 (3.95e-4)	1.55e-3 (3.48e-4)	3.10e-3 (6.65e-4)
LD6-5412	128	--	1,030	41.9	7.48e-4 (1.53e-4)	--	2.44e-3 (5.38e-4)
LD6-5412	45	--	955	59.0	1.45e-4 (4.40e-5)	--	2.19e-3 (4.89e-4)
LD6-5412	40	--	933	82.1	1.08e-4 (3.76e-5)	--	2.05e-3 (4.68e-4)
HLP-33	302	255	3,240	3.2	6.15e-3 (1.16e-3)	5.82e-3 (1.10e-3)	7.56e-3 (1.36e-3)
HLP-33	197	169	2,730	11.5	3.85e-3 (6.90e-4)	3.67e-3 (6.78e-4)	6.19e-3 (1.12e-3)
HLP-33	171	152	2,710	21.3	3.29e-3 (6.16e-4)	3.26e-3 (6.31e-4)	6.20e-3 (1.10e-3)
HLP-33	100	112	2,570	39.2	1.69e-3 (3.63e-4)	2.23e-3 (4.43e-4)	5.78e-3 (1.04e-3)
HLP-33	92	110	2,370	57.7	1.49e-3 (3.10e-4)	2.13e-3 (4.34e-4)	5.14e-3 (9.67e-4)
HLP-33	59	88	2,270	76.7	7.79e-4 (2.12e-4)	1.62e-3 (3.57e-4)	4.97e-3 (9.93e-4)
BAS-1	--	1020	29,100	21.3	--	3.29e-2 (6.99e-3)	1.01e-1 (2.15e-2)
BAS-1	--	2140	38,100	55.3	--	6.92e-2 (1.47e-2)	1.32e-1 (2.80e-2)
BAS-1	--	2250	39,300	67.1	--	7.45e-2 (1.58e-2)	1.39e-1 (2.95e-2)
BAS-1	--	2110	36,100	82.3	--	6.93e-2 (1.47e-2)	1.27e-1 (2.70e-2)
BAS-1	--	1660	34,100	91.9	--	5.50e-2 (1.17e-2)	1.21e-1 (2.58e-2)
BAS-1	--	1720	33,500	110.0	--	5.66e-2 (1.20e-2)	1.18e-1 (2.51e-2)

The elemental release data are consistent with release of Na by two distinct mechanisms: a) release due to Na^+—H^+ ion exchange (or IEX), and b) liberation through hydrolysis and dissolution of the glass network. As discussed above, quantification of the IEX rate was accomplished by subtracting the matrix dissolution rate, represented by the Al or B release rate, from the Na release rate. IEX rates are listed in Table III.

Table III. Rates of Na Ion Exchange for Borosilicate Glasses at 40°C, *p*H(25°C) = 8 and Silica Saturation

Glass I.D.	IEX rate mol/(m^2·s)	IEX error mol/(m^2·s)
LAWABP1	1.66E-10	3.68E-11
LAWA33	9.48E-11	4.15E-11
LAWA44	1.75E-11	5.93E-11
LD6-5412	2.28E-10	1.47E-10
HLP-9	7.81E-11	4.58E-11
HLP-12	3.73E-11	1.07E-10
HLP-33	2.93E-10	9.22E-11
BAS-1	5.13E-09	2.32E-09
HAN-28F	2.00E-09	4.81E-10

It is clear that the magnitude of IEX rate varies amongst the various glasses. Theoretically, these differences in IEX rate should be proportional to the number of Na atoms associated with NBO's in the disrupted Si—O—Al network. In the model of Dell et al. [20], for every atom of Na beyond that which can be balanced by an equivalent number of Al^{3+} or B^{3+} atoms results in the formation of an NBO site. The sodium atoms associated with NBO sites are more vulnerable to IEX reactions than those associated with BO sites. Accordingly, the greater proportion of NBO to BO sites, the greater the magnitude of Na release by IEX. Although it is possible to characterize the number of NBO sites in glass using spectroscopic techniques, a simpler (though, likely less accurate) way to predict the magnitude of the IEX reaction is to examine the molar ratio of Na to the sum of charge-compensating cations [see Equation (2)], such as Al^{3+}, B^{3+} and Fe^{3+}. Although the fraction of Fe^{3+}/Fe^{2+} has not been determined in the more complex glasses tested in this investigation, spectroscopic work suggests that most of the iron is Fe^{3+} [20]. Accordingly, on a plot of molar $Na/\Sigma(Al^{3+}, B^{3+}, Fe^{3+})$ (or *R*), there should be a positive correlation with IEX rate. Figure 3 shows that there is a strong correlation between these parameters. A regression of a line through the data yields the following equation:

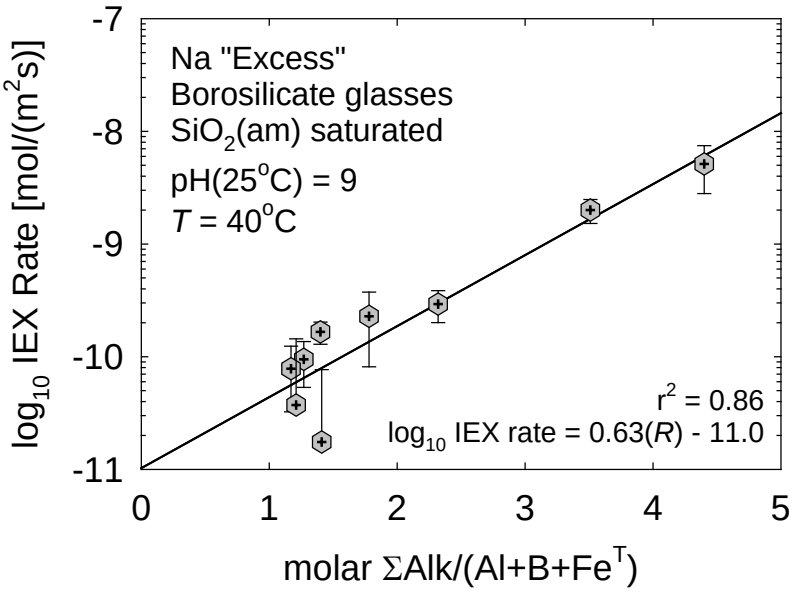

Figure 3. Plot of $\log_{10}$ Na-H ion exchange rate versus the molar ratio of alkali elements to network-forming elements. The line of correlation indicates that glass chemistry controls the IEX rate.

$$\log_{10}\text{rate}[\text{mol}/(\text{m}^2\cdot\text{s})] = 0.63R + (-11.0);\ r^2 = 0.86 \qquad \text{(Eq. 6)}$$

where rate is the flux of Na (meter squared per second). Because of the wide variation in glass chemistries, it is likely that this equation will be valid for most aluminoborosilicate glass in which there is excess Na.

2. Dissolution in Silica-Amended D_2O Solutions. Dissolution kinetics of the borosilicate glasses is presented in Table IV. Release of glass network-forming constituents, such as Al and B, are the same in H_2O as compared to D_2O. These results are expected because the network hydrolysis reaction is not subject to isotopic effects involving H—D. On the other hand, release rates of Na are quantitatively slower in D_2O compared to H_2O. These results concur with those from earlier studies—sodium trisilicate glass [12] and sodium aluminosilicate glasses [16]—and are indicative of a difference of average vibrational energy between H and D bonded to oxygen.

As explained by Pederson [12], rates of reaction are proportional to the vibrational frequencies of the principal chemical bonds:

$$\nu = (1/2)\pi(k_{1,2}/m)^{1/2} \qquad \text{(Eq. 7)}$$

in which $k_{1,2}$ is the force constant of the critical bond and m is the reduced mass. The "critical bond" is that of O—H. Accordingly, the relative rate of Na release in D_2O compared to that in H_2O is:

Table IV. Concentrations of B, Na and Si with Corresponding Release Rates in Either H_2O or D_2O, T = 40°C, pH = pD = 8 and at Silica Saturation.

Glass I.D. (matrix)	Conc. B (μg/L)	Conc. Na (μg/L)	Conc. Si (mg/L)	rate B [g/(m^2·d)]	rate Na [g/(m^2·d)]
HLP-9 (H_2O)	43	939	95.6	6.46e-4 (3.00e-4)	3.70e-3 (7.27e-4)
HLP-9 (D_2O)	50	169	70.8	7.96e-4 (3.59e-4)	7.60e-4 (1.84e-4)
HLP-12 (H_2O)	50	902	95.6	9.97e-4 (2.25e-4)	3.66e-3 (7.23e-4)
HLP-12 (D_2O)	50	228	75.4	9.90e-4 (2.23e-4)	1.02e-3 (2.32e-4)
LAWA33 (H_2O)	50	606	95.7	1.08e-3 (2.44e-4)	2.35e-3 (4.99e-4)
LAWA33 (D_2O)	50	300	70.4	1.08e-3 (2.44e-4)	1.26e-3 (3.02e-4)
LAWA44 (H_2O)	50	780	96.4	1.08e-3 (1.91e-4)	3.02e-3 (1.19e-3)
LAWA44 (D_2O)	50	459	56.2	1.08e-3 (2.33e-4)	1.76e-3 (7.08e-4)
LD6-5412 (H_2O)	50	1317	94.7	1.92e-3 (2.54e-4)	4.93e-3 (1.92e-3)
LD6-5412 (D_2O)	50	283	69.6	1.93e-3 (8.69e-4)	1.20e-3 (5.32e-4)
LAWABP-1 (H_2O)	50	742	94.9	1.04e-3 (4.67e-4)	2.69e-3 (1.10e-3)
LAWABP-1 (D_2O)	50	277	65.2	1.03e-3 (4.66e-4)	1.18e-3 (5.68e-4)

$$k(D_2O) = k'(H_2O)(m_H/m_D)^{1/2} \qquad \text{(Eq. 8)}$$

in which k is the rate of release and k' is the rate constant. Thus, the difference in rate is calculated to be 0.71. In Table IV, the relative difference between rates in D_2O is at least 30% less than in H_2O, which is evidence for Na IEX reactions, and also for the involvement of H^+ (or D^+).

The involvement of H^+ (or D^+) species in an IEX reaction is unlikely, because of the high degree of reactivity of H^+, as discussed by Pederson [12]. In an earlier paper [16], we argued that molecular water was implicated as the primary hydrogen-bearing species in the reaction layer of

the sodium aluminosilicate glasses. A likely scenario for the involvement of hydrogen is that molecular water diffuses into the glass and comes in contact with Na atoms. Water is de-protonated and the H^+ then exchanges with Na^+ in the glass structure. Sodium is then free to diffuse from the glass and into aqueous solution. In this scenario, the rate-limiting kinetic step is the rupture of the H—O bond in the water molecule.

DISCUSSION

Exchange of Na^+ from glass for hydrogen species from aqueous solution has mainly been considered as important only in the initial stages of glass reactivity. On the other hand, Ojovan et al. [17] and McGrail et al. [16] have suggested that this mechanism may be important in later stages of glass corrosion as well. Because the IEX reaction is not influenced by chemistry of the aqueous solution with which it is in contact (either solution saturation state or the concentration of Na^+ in solution), this mechanism will continue to release Na^+ to solution over the duration of the glass/water reaction. As hydrolysis and matrix dissolution becomes the dominant element release mechanisms, the contribution of Na^+ released by IEX will be small compared to that of the former. However, in environments in which Si builds up in solution adjacent to glass (such as when water percolates slowly through the disposal vault), the glass dissolution reaction decreases in response to the chemical affinity of the reaction. If the matrix dissolution rate decreases below that of the IEX, then the latter will become the dominant mechanism that liberates Na^+ to solution. Depending on the magnitude of the surface area in contact with aqueous solution, and the volume of solution, the pH of solution will increase, creating a classic feedback mechanism between IEX and glass dissolution. Therefore, the action of IEX in Na-rich glasses may result in a "buffering" of the dissolution rate to relatively fast rates.

The relevance of this model is that there has been discussion in the literature regarding the long-term rate of aluminosilicate minerals and glasses and their relationship to rates determined in the laboratory. For example, White and Brantley [9] argued that dissolution rates of silicate minerals obtained by laboratory experiment are 2 to 6 orders-of-magnitude faster than those determined in the field. Part of the reason for this discrepancy is the complex evolution of reactive surface area as weathering proceeds [9]. In addition, most experiments are conducted in dilute solutions, whereas those in sedimentary environments are closer to saturation with respect to rate-limiting secondary phases. Consonant with these arguments, Gordon and Brady [8] argued that basaltic glass also dissolved at much slower rates than those inferred from laboratory experiments. Because natural basaltic glass bears some similar chemical traits to that of waste glass, they suggested that the latter may dissolve more slowly than suspected. In sum, these two studies could be construed to give more credit to the chemical durability of borosilicate waste glass than is currently given. However, the results of this investigation indicate that this is unlikely to be the case for Na-rich borosilicate glass. Because of the excess of Na with respect to charge-compensating cations such as Al, B, and Fe, IEX reactions will dominate glass corrosion behavior in near silica-saturated environments. The IEX reactions will cause a feedback mechanism in which solution pH is high, resulting in faster release of glass constituents. Therefore, we expect that basaltic glass, which does not have excess Na (at least not those tested by Gordon and Brady), will behave very differently than Na-rich borosilicate waste glass.

In order to evaluate this idea, we looked in the literature for "field rates" of Na-rich glass. Varlakova and Semenov [21] reported laboratory rates for the Russian K-26 glass determined both under dilute and silica-rich conditions. In dilute solutions, the K-26 glass at 17°C dissolved at a rate of 2.23×10^{-13} mol/(cm^2·s), and in a solution containing 58.6 ppm Si dissolved at 9.19×10^{-14} mol/(cm^2·s). In other words, the addition of Si to solution resulted in a decrease of a factor of 2.4× compared to the dilute experiment. Ojovan et al. [11] tested the same glass in a lysimeter

and found the dissolution rate to be 1.79×10^{-14} mol/(cm^2·s) after one year's reaction time, consistent with the laboratory rates. After 16 years of testing, the field rate was measured as 4.20×10^{-15} mol/(cm^2·s). So, the difference in rate between the first and sixteenth year is only a factor of 4.3×. This difference is about the same between the laboratory dilute and Si-amended rates. Even when comparing the slowest field [4.20×10^{-15} mol/(cm^2·s)] and the fastest laboratory [2.23×10^{-13} mol/(cm^2·s)] rates the difference is about a factor of 53×. In comparison, the dissolution rate of fresh Panola Granite was reported as 7.0×10^{-14} mol/(m^2·s), and the field-determined rate was 2.8×10^{-16} mol/(m^2·s), or a factor of 250× slower [9]. This factor is clearly much larger than that measured for the Russian K-26 glass.

Part of the problem in interpreting these results is that the rate obtained on the Panola Granite was based on exposure to dissolution of up to 350 000 years. It may not be valid, therefore, to compare the results of experiments and the relatively short-term lysimeter tests cited above. On the other hand, a set of experiments in which reaction rates were greatly accelerated, may shed some light on the change in rate over time. The Pressurized Unsaturated Flow (PUF) test is designed to mimic conditions of partial hydraulic saturation at elevated temperatures. The salient features of this experimental apparatus and a discussion of its workings are presented in [22-24]. For the purposes of this discussion, the relevant information is that the PUF test causes an increase in the dissolution rate by a factor of 50×, and this is due to the small volume of water into which the glass dissolves. When the hydraulic saturation is low, the aqueous solution forms a thin film on the surface of the glass particles, so IEX reactions can potentially become important and may prevent dissolution rates from decreasing below a threshold value.

PUF experiments on borosilicate glass carried out by Pierce et al. [23] were conducted for approximately 6 years. Because the PUF test accelerates the rate of reaction by ~50×, the glass samples were subjected to an equivalent of ~300 years of testing, which would be a long enough time interval to observe a steady decrease in rate over the duration of the experiment. In contrast to these expectations, the documented glass dissolution rates (based on Li and Si release) decreased in the first year and then reached steady-state values over the remainder of the test. Clearly, a mechanism or mechanisms prevented a steady, observable decrease in dissolution rates. Experiments conducted for shorter periods of time (~1.5 years) on two sodium-excess boroaluminosilicate glasses also showed a slight decrease in rate followed by an approach to constant rate values near the end of the experiments. In these experiments, the normalized release of Na was much faster than that of the network forming elements, Si and Al, indicating that IEX reactions were active. However, it should be noted that rates of element release were also subject to formation of secondary phases. As discussed by Pierce et al. [23], the precipitation of secondary phases may cause the activities of key elements (e.g., Al, Si) that affect the solution saturation state to diminish, causing the glass dissolution rates to increase, or at least to not fall below a certain value. Therefore, although IEX reactions may not be solely responsible for "buffering" the dissolution rates at a constant value, the lysimeter and PUF data indicates that there is no reason to believe that long-term rates undergo drastic decreases in dissolution rate, as in the case of silicate minerals and common (no excess Na) glasses. The presence of "excess" Na in borosilicate glass may prevent a 2- to 6-orders-of-magnitude drop in dissolution rates; accordingly, credit for a sharp decrease in radioactive element release from glass in the long-term may not be warranted and is discouraged.

REFERENCES

1. T. ADVOCAT, P. JOLLIVET, J. L. CROVISIER, and M. DEL NERO, "Long-Term Alteration Mechanisms in Water for SON68 Radioactive Borosilicate Glass", *Journal of Nuclear Materials*, 298: 55-62 (2001).
2. W. L. BOURCIER, D. W. PEIFFER, K. G. KNAUSS, K. D. MCKEEGAN, and D. K. SMITH, "A Kinetic Model for Borosilicate Glass Dissolution Based on the Dissolution Affinity of a Surface Alteration Layer", in *Scientific Basis for Nuclear Waste Management XIII*, V. M. OVERSBY and P. W. BROWN, Eds., Materials Research Society: Pittsburg, PA, 209-216 (1990).
3. E. CURTI, J. L. CROVISIER, G. MORVAN, and A. M. KARPOFF, "Long-Term Corrosion of Two Nuclear Waste Reference Glasses (MW and SON68): A Kinetic and Mineral Alteration Study", *Applied Geochemistry*, 21: 1152-1168 (2006).
4. G. LETURCQ, G. BERGER, T. ADVOCAT, and E. VERNAZ, "Initial and Long-Term Dissolution Rates of Aluminosilicate Glasses Enriched with Ti, Zr and Nd", *Chemical Geology*, 160: 39-62 (1999).
5. P. VAN ISEGHEM and B. GRAMBOW, "The Long-Term Corrosion and Modelling of Two Simulated Belgian Reference High-Level Waste Glasses", in *Scientific Basis for Nuclear Waste Management XI*, M. J. APTED and R. E. WESTERMAN, Eds., Materials Research Society: Pittsburgh, PA, 631-639 (1988).
6. P. AAGAARD and H. C. HELGESON, "Thermodynamic and Kinetic Constraints on Reaction Rates among Minerals and Aqueous Solutions. I. Theoretical Considerations", *American Journal of Science*, 282: 237-285 (1982).
7. R. H. DOREMUS, "Interdiffusion of Hydrogen and Alkali Ions in a Glass Surface", *Journal of Non-Crystalline Solids*, 19(2): 137-144 (1977).
8. S. J. GORDON and P. V. BRADY, "In situ Determination of Long-Term Basaltic Glass Dissolution in the Unsaturated Zone", *Chemical Geology*, 190: 113-122 (2002).
9. A. F. WHITE and S. L. BRANTLEY, "The Effect of Time on the Weathering of Silicate Minerals: Why do Weathering Rates Differ in the Laboratory and Field?", *Chemical Geology*, 202: 479-506 (2003).
10. B. P. MCGRAIL, D. H. BACON, J. P. ICENHOWER, F. M. MANN, R. J. PUIGH, H. T. SCHAEF, and S. V. MATTIGOD, "Near-Field Performance Assessment for a Low-Activity Waste Glass Disposal System: Laboratory Testing to Modeling Results", *Journal of Nuclear Materials*, 298: 95-111 (2001).
11. M. I. OJOVAN, R. J. HAND, N. V. OJOVAN, and W. E. LEE, "Corrosion of Alkali-Borosilicate Waste Glass K-26 in Non-Saturated Conditions", *Journal of Nuclear Materials*, 340: 12-24 (2005).
12. L. R. PEDERESON, "Comparison of Sodium Leaching Rates from a $Na_2O{\cdot}3SiO_2$ Glass in H_2O and D_2O", *Physics and Chemistry of Glasses*, 28(1): 17-21 (1987).
13. D. R. BAER, L. R. PEDERSON, and G. L. MCVAY, "Glass Reactivity in Aqueous Solutions", *Journal of Vacuum Science Technology*, A 2(2): 738-743 (1984).
14. L. R. PEDERSON, D. R. BAER, G. L. MCVAY, K. F. FERRIS, and M. H. ENGELHARD, "Reaction of Silicate Glasses in Water Labeled with D and ^{18}O", *Physics and Chemistry of Glasses*, 31: 177-182 (1990).
15. L. R. PEDERSON, D. R. BAER, G. L. MCVAY, and M. H. ENGELHARD, "Reaction of Soda Lime Silicate Glass in Isotopically Labeled Water", *Journal of Non-Crystalline Solids*, 86: 369-380 (1986).
16. B. P. MCGRAIL, J. P. ICENHOWER, D. K. SHUH, P. LIU, J. G. DARAB, D. R. BAER, S. THEVUTHASEN, V. SHUTTHANANDAN, M. H. ENGELHARD, C. H.

BOOTH, and P. NACHIMUTHU, "The Structure of Na_2O-Al_2O_3-SiO_2 Glass: Impact on Sodium Ion Exchange in H_2O and D_2O", *Journal of Non-Crystalline Solids*, 296: 10-26 (2001).

17. M. I. OJOVAN, A. PANKOV, and W. E. LEE, "The Ion Exchange Phase in Corrosion of Nuclear Waste Glasses", *Journal of Nuclear Materials*, 358(1): 57-68 (2006).
18. B. GRAMBOW, "A General Rate Equation for Nuclear Waste Glass Corrosion", in *Scientific Basis for Nuclear Waste Management VIII*, C. M. JANTZEN, J. A. STONE, and R.C. EWING, Eds., Materials Research Society: Pittsburg, PA, 15-27 (1985).
19. W. J. DELL, P. J. BRAY, and S. Z. XIAO, "^{11}B NMR Studies and Structural Modeling of Na_2O-B_2O_3-SiO_2 Glasses of High Soda Content", *Journal of Non-Crystalline Solids*, 58(1): 1-16 (1983).
20. M. WILKE, G. M. PARTZSCH, R. BERNHARDT, and D. LATTARD, "Determination of the Iron Oxidation State in Basaltic Glasses using XANES at the K-edge", *Chemical Geology*, 220: 143-161 (2005).
21. G. A. VARLAKOVA and K. N. SEMENOV, "Long-Term Testing and Prediction of Glass Performance-Russian Experience at Burial Site", SUE SPA RADON: Moscow, Russia (2005).
22. B. P. MCGRAIL, P. F. MARTIN, C. W. LINDENMEIER, and H. T. SCHAEF, "Application of the Pressurised Unsaturated Flow (PUF) Test for Accelerated Ageing of Waste Forms", in *Ageing Studies and Lifetime Extension of Materials*, L. G. MALLISON, Ed., Kluwer Academic/Plenum Publishers: New York, NY, 313-320, (2001).
23. E. M. PIERCE, B. P. MCGRAIL, P. F. MARTIN, J. MARRA, B. W. AREY, and K. N. GEISZLER, "Accelerated Weathering of High-Level and Plutonium-Bearing Lanthanide Borosilicate Waste Glasses under Hydraulically Unsaturated Conditions", *Applied Geochemistry*, 22: 1841-1859 (2007).
24. E. M. PIERCE, B. P. MCGRAIL, M. M. VALENTA, and D. M. STRACHAN, "The Accelerated Weathering of a Radioactive Low-Activity Waste Glass under Hydraulically Unsaturated Conditions: Experimental Results from a Pressurized Unsaturated Flow Test", *Nuclear Technology*, 155: 149-165 (2006).